



Porous Methylsilsequioxane for Low-*k* Dielectric Applications

Agnes M. Padovani,^a Larry Rhodes,^b Laura Riester,^c Gregory Lohman,^b
Barbara Tsuie,^a James Conner,^d Sue Ann Bidstrup Allen,^a and Paul A. Kohl^{a,*}

^aSchool of Chemical Engineering, Georgia Institute of Technology, Atlanta, Georgia 30332-0100, USA

^bGoodrich Corporation, Brecksville, Ohio 44141, USA

^cOak Ridge National Laboratory, Oak Ridge, Tennessee 37831-6069, USA

^dMotorola Incorporated, Austin, Texas 78721, USA

A commercially available spin-on glass (methylsilsequioxane, MSQ) was modified by the introduction of porosity. The porosity reduced the effective dielectric constant of the MSQ by the incorporation of air. The pores were created by adding a sacrificial polymer (substituted norbornene polymer) to the silsequioxane matrix. The sacrificial material was thermally decomposed to form nanosize voids within the films. The physical and electrical properties of the porous films were studied as a function of the reactivity of the sacrificial polymer with the glass, and the loading and molecular weight of the sacrificial polymer. Transmission electron microscopy was used to evaluate the porous microstructure. Cross-sectional images show pores of nearly spherical geometry with 5-20 nm diam. The dielectric constant and the index of refraction of the porous MSQ were lower after the decomposition of the sacrificial material. The dielectric constant decreased from 2.7 for a nonporous MSQ film to ~2.2 for a film with 30 wt % loading of the sacrificial polymer. In a similar way, the index of refraction was reduced from 1.42 to 1.29 for the porous MSQ film. The mechanical properties were evaluated using nanoindentation techniques. This paper focuses on the significant improvements observed upon introduction of porosity to the films. The fracture toughness, or the resistance to crack propagation, increased dramatically with porosity, as compared with the nonporous MSQ films. As a result, thicker MSQ films can be fabricated without spontaneous cracking. The elastic modulus and the hardness of the porous films were measured and showed a reduction in both properties with increasing porosity in the film.

© 2001 The Electrochemical Society. [DOI: 10.1149/1.1403215] All rights reserved.

Manuscript submitted April 24, 2001; revised manuscript received July 7, 2001. Available electronically August 24, 2001.

To meet the increasing demand for smaller, faster, and more powerful electronic devices, the International Technology Roadmap for Semiconductors¹ (ITRS) predicts the dielectric constant of the interlevel metal insulator needs to be approximately 2.0 by the year 2003. This is due to the need for lower interconnect delay to enable higher device speeds, especially as the critical dimensions are lowered below 0.13 μm . The delay can be characterized by the resistance-capacitance coupling (RC time constant) in the interconnects. Two materials changes are being made to mitigate the problem; the use of lower resistivity metals (*e.g.*, copper) that would reduce resistance, and the use of lower dielectric constant insulators to lower capacitance. There are several options for low-*k* insulators, such as fluorinated and carbon-doped silica glasses and organic polymers.² However, despite their reduced dielectric constant, when compared to silicon dioxide, none of these fully densified materials has a dielectric constant low enough for future interconnections. Porous materials can meet the low dielectric constant objectives of the ITRS; however, the method of fabrication and impact on properties is critically important. For a porous material, the low dielectric constant is the result of mixing air with the solid phase. There are other advantages in using porous dielectrics, besides the low-*k*, such as being able to use the same material for an additional device generation by the introduction of porosity. This would avoid major material-related process changes, and reduce the time to market of the new product.

There are significant issues associated with using porous films as dielectric layers for microelectronic applications. Many issues deal with pore size and distribution, and control over the pore parameters. To assure proper device operation, a porous dielectric film would need to have a homogeneous pore distribution with sizes that are 10% or less of the smallest feature size. In terms of the processing conditions, this would require tight control over the pore size and a narrow size distribution. It is also desirable to have closed-cell pores to inhibit diffusion or migration of contaminants. Finally, the mechanical properties of the porous materials are of great concern because of the possible impact on the other fabrication processes and device lifetime.

This study reports on the formation of porous methylsilsequioxane (MSQ, $\text{CH}_3\text{SiO}_{1.5}$) films through the use of a template technique similar to the one described by Hedrick *et al.* (1998).³ This technique uses two materials, a main dielectric matrix and a sacrificial material that is thermally decomposed to form nanosize voids within the matrix film. During thermal treatment, the decomposition products volatilize and permeate through the main matrix, thus creating free volume within the films (air diffuses in from the opposite direction). The template technique creates the voids at sites occupied by the sacrificial material prior to the decomposition process, so that by controlling the dispersion or the distribution of one material within the other, the resulting microstructure can be tailored. This study controls the porosity and distribution of pores by chemically bonding the sacrificial material to the matrix. The chemical reaction between the matrix and the sacrificial material avoids phase separation or agglomeration of sacrificial material, because this would ultimately lead to the formation of larger pores.

In this study, commercially available MSQ was made porous by the use of substituted norbornene polymers (PNB) as the sacrificial material. The use of these polymers for sacrificial templating has been previously demonstrated through the formation of air gaps.⁴ Two functional groups, trimethoxysilyl and triethoxysilyl, were used as substituents on the norbornene backbone to test the difference in chemical bonding with the spin-on glass matrix. Upon hydrolysis, the methoxy- or ethoxysilyl groups convert into silanol (-Si-OH) moieties. Because the cure process of the MSQ also involves silanol groups that condense to form a network structure, the condensation of the MSQ with the PNB also occurred. With this approach, PNB molecules could be bonded at specific sites within the MSQ matrix. The selectivity of the chemical reactions, and the temperature (and other conditions) under which these reactions occur, are being investigated.

Experimental

Honeywell 418 MSQ (Santa Clara, CA) was made porous by the use of two different sacrificial materials. Triethoxysilyl and trimethoxysilyl norbornene homopolymers (Mw ~40,000), (Atrium sacrificial polymers, BFGoodrich, Brecksville, OH) were used. Triethoxysilyl norbornene (TESNB) had been previously shown useful as a sacrificial place-holder (template) in spin-on glasses.⁵ The solutions were prepared by initially dissolving at 20 wt % both the

* Electrochemical Society Active Member.

^z E-mail: paul.kohl@che.gatech.edu

MSQ and the sacrificial polymers in methyl isobutyl ketone, MIBK. The MSQ resin was redissolved in MIBK after evaporating the original solvent (a mixture of methanol, ethanol, and butanol). This was necessary to avoid solvent incompatibilities that could induce phase separation upon mixing. The mixtures were prepared by combining MSQ with 0-30 wt % (MSQ basis only, solvent not considered) of either TESNB or trimethoxysilyl norbornene (TMSNB). The mixtures were spin-coated onto 100 mm silicon <100> wafers at spin speeds from 600-2000 rpm, to obtain a thickness between 300 and 1200 nm. The thickness was measured using both a Dektak profilometer and a variable angle spectroscopic ellipsometer (VASE, J. A. Woollam Co., Inc.). The films were cured, as suggested by the vendor,⁶ using a sequence of hot plates at 180°C for 2 min, and 250°C for 1 min, followed by a furnace cure with nitrogen purge. The furnace was ramped at 3°C/min to 425°C, and held at that temperature for 1.5 h before cooling to room temperature. The high-temperature treatment was necessary to fully cure the MSQ into a network structure, which fully condenses the silanol groups into Si-O-Si bonds, and to decompose the PNB within the films. Transmission electron microscopy (TEM) was used to study the resulting microstructure, pore size, and distribution. Ultrathin cross sections (~100 nm) of the porous films, appropriate for TEM investigation, were prepared using focused ion beam (FIB) techniques performed at Motorola. Dielectric constant measurements were performed by preparing metal-insulator-metal (MIM) structures, and measuring the capacitance between the parallel plate electrodes at a frequency of 10 kHz. For these experiments, spin-on glass films were cast onto metallized silicon substrates. The top electrode consisted of sputtered Al (2000 Å), and was patterned by photolithography (1.5 mm diam capacitors). The index of refraction of the porous films was measured using a single wavelength ellipsometer at 70° incidence angle and 632.8 nm wavelength. Nanoindentation experiments, performed at Oak Ridge National Laboratory, were used to evaluate the mechanical properties of the porous films. The instrument used was a Nano Indenter II by Nano-Instruments, Inc. (Oak Ridge, TN). The elastic modulus and the hardness were calculated from the data for the hold segments of a continuous stiffness experiment⁷ using a Berkovich tip. A total of ten indents were made per sample, each consisting of three penetration-hold segments. The penetration depths were fixed at 25, 50, and 75 nm to avoid the effect of the underlying silicon substrate in the measurements. To evaluate the fracture toughness, or the resistance to crack propagation in the films, a different experiment was performed using a cube-corner tip geometry. For this study, five indents at each of six different loads ranging from 0.01 to 10 mN were made per sample. After the indentation process, scanning electron microscopy (SEM) was used to measure the length of the cracks propagating from the corners of the impressions.

Results and Discussion

Figure 1 shows a cross-sectional TEM of a 20:80 wt % TMSNB:MSQ film after decomposition of the sacrificial material. The lighter (less electron dense) regions in the images (Fig. 1, bottom) correspond to the porosity. The results show that the pores are nearly spherical in shape with diameters of 3-10 nm. As a first indication, the porosity appears to be closed-cell; there does not appear to be intersecting pores. The initial positronium annihilation lifetime spectroscopy (PALS)⁸ and Doppler broadening positron spectroscopy⁹ studies support the existence of closed pores at lower loadings. These results will be reported in a later publication.

The pore diameter as a function of sacrificial loading level is a critical parameter. Films were prepared with a TMSNB:MSQ ratio of 0:100, 10:90, 20:80, 30:70, and 40:60. The results show that the pore size is similar (3-10 nm), and independent of the loading level. Increasing the amount of sacrificial polymer in the sample does increase the pore density (number of pores per volume) in the film, but does not affect the pore size. Larger pores were not observed at 40 wt % load of TMSNB. A possible explanation for this behavior suggests that proper mixing and chemical bonding at the molecular

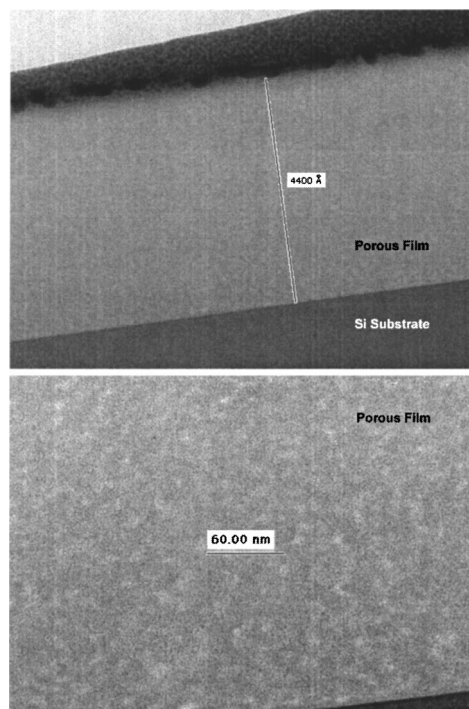


Figure 1. TEM images for a 20:80 wt % TMSNB:MSQ film after decomposition.

level was achieved even at the higher loads, thus minimizing phase separation and agglomeration of the polymer. The chemical bonding of the porogen (PNB) with the spin-on glass is being studied with solid-state ²⁹Si and ¹³C nuclear magnetic resonance (NMR) spectroscopy and Fourier transform infrared (FTIR) analysis.

The index of refraction and dielectric constant of TMSNB:MSQ mixtures are shown in Fig. 2. Both properties show a monotonic decrease with TMSNB loading due to the higher degree of porosity. In Fig. 2, it was assumed that the porosity was linearly related to the PNB content. The void fraction was calculated from the estimated solid densities of MSQ and PNB, assuming the volume of the pores to be the same as the volume occupied by the PNB before the decomposition process. In this case, a 40:60 wt % TMSNB:MSQ film would be expected to have 43.4% (by volume) porosity.

The results for the dielectric constant measurements show a reduction from $\epsilon_r = 2.68$ for a nonporous MSQ film, to $\epsilon_r = 2.24$ for a porous film of 30:70 wt % TMSNB:MSQ (after decomposition). The result for the pure MSQ film agrees with the reported value of 2.7 at 1 MHz. The values for the porous films were compared with those calculated for binary mixtures using the equations presented by Jayasundere *et al.*¹⁰ The numbers were calculated by using the estimated volume fractions and the respective dielectric constants of

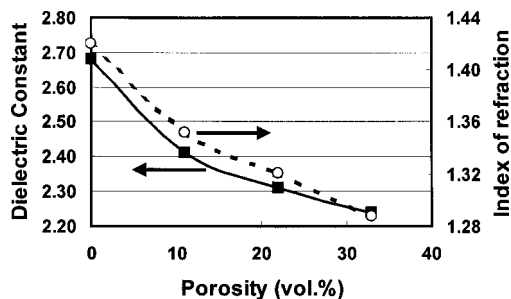


Figure 2. Measured dielectric constant and index of refraction as a function of the estimated porosity in the films.

2.7 and 1.0 for a mixture of MSQ and air. For a 20:80 wt % TMSN:MSQ film, the measured dielectric constant was 2.31 (an average over ~30 capacitors), and the calculated value was 2.29. This shows a difference of only 1% between the theoretical and experimental values. Further, the dielectric constant was calculated using the approach used by Xu *et al.*¹¹ to estimate the porosity of an ultralow-*k* dielectric material. In their study, a logarithmic mixing rule was used for the dielectric constant. With this equation, a film of 10:90 wt % TMSN:MSQ after decomposition would have a dielectric constant of 2.40. The measured value for this system was 2.41. These results are comparable to a previous report on porous MSQ using poly(ϵ -caprolactone) as the porogen.¹² Dielectric constants of about 2.55, 2.25, and 2.0 were reported with 10, 20, and 30 wt % porogen, respectively.

Similarly, the results for the index of refraction show a reduction from 1.42 for an MSQ film to 1.29 for a 30:70 wt % TMSN:MSQ film after heat-treatment. The results were compared with the values obtained from the mixing rules. A linear mixing rule was used for comparison. For samples of 20:80 and 30:70 wt % TMSN:MSQ, the measured index values were 1.32 and 1.29, respectively. The calculated values for these same mixtures were 1.33 and 1.28, a difference of only 0.4% between the theoretical and experimental values. These results, along with the dielectric constant values, demonstrate the good optical and electrical properties of the porous films made using this sacrificial polymer approach.

The mechanical properties of porous materials are critical in the integration capability of these films. Nanoindentation experiments were performed to characterize the mechanical properties. Figure 3 shows an array of indents made to study the resistance to crack propagation of the films. The experiments were performed at 10, 2, 1, 0.5, 0.1, and 0.01 mN of force. Figure 3a shows indents at 10, 2, 1, and 0.5 mN force (left to right). The 0.1 and 0.01 mN indents were totally elastic and therefore are not visible in Fig. 3a (no plastic deformation or cracking occurred). Five repetitions of each indent are shown in Fig. 3a from top to bottom. It is important to note that each indent was made in a single load-unload segment. That is, the indenter penetrated the surface once with the specific applied force, and then immediately unloaded. Figure 3b corresponds to a film of 90:10 wt % MSQ with TESNB as the sacrificial polymer. The array of indents in this image was made exactly the same way as in the MSQ sample, with the only difference that only four repetitions (top-to-bottom) are shown. In the last row (fifth from the top), every indent was made at 10 mN force. The dramatic contrast between the cracks in Fig. 3a and b depicts the remarkable improvement in the mechanical properties of the films with the introduction of porosity. In the MSQ films, Fig. 3a, the cracks extended all the way to the edge of the wafer. With the porous films, the cracks did not propagate beyond the point of indentation. From Fig. 3b it is clear that some plastic deformation occurred in both films because the impressions were retained after the indentation process. Pure MSQ is known to be susceptible to cracking due to the intrinsic stress in the film. The difference between MSQ and fully relaxed silicon dioxide lies with the bond-strain in MSQ, where each silicon atom is bonded to 1.5 oxygen atoms, and one nonbridging CH₃ group. The effect of the intrinsic strain in these bonds imposes a thickness limit on these films. It is difficult to fabricate MSQ films thicker than about 600 nm because they crack upon processing. Although the films in Fig. 3 were below the cracking threshold for MSQ (films of ~400 nm), the indentation process induced cracking. The crack propagation relieved the intrinsic stress in the films.

A quantitative measure of the results observed with these samples (cracks vs. no cracks) is presented in Fig. 4. The average fracture toughness as a function of the initial concentration of sacrificial TESNB is shown in Fig. 4. The values were the average of 30 indentations in each sample at the applied forces mentioned before. The results are also shown as a function of the average thickness of the films.

The fracture toughness was calculated using Eq. 1

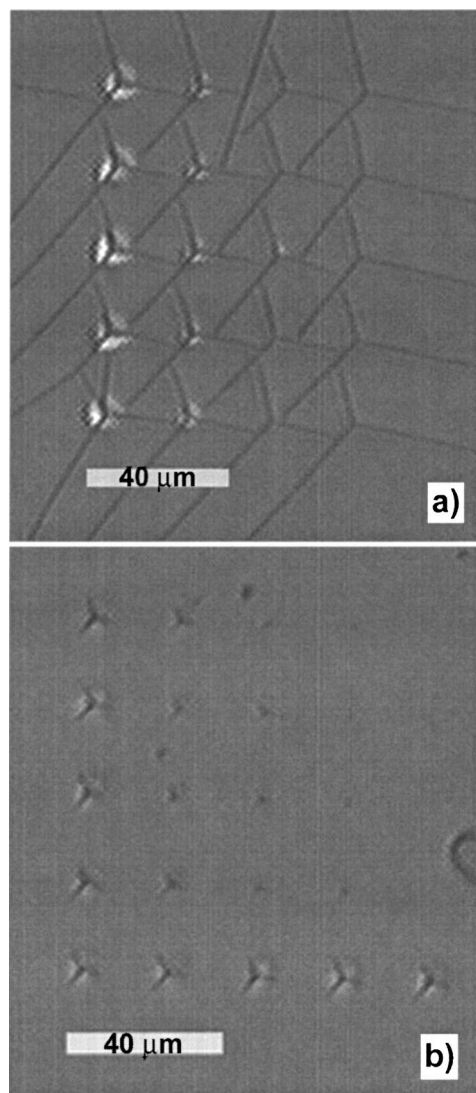


Figure 3. Fracture toughness indents for an (a) MSQ film and (b) 10:90 wt % TESNB:MSQ film.

$$K_c = \alpha \left(\frac{E}{H} \right)^{1/2} \left(\frac{P}{c^{3/2}} \right) \quad [1]$$

where K_c is the fracture toughness, α is an empirical constant dependent on the tip geometry, E is the elastic modulus, H is the hardness, P is the peak indentation load, and c is the length of the

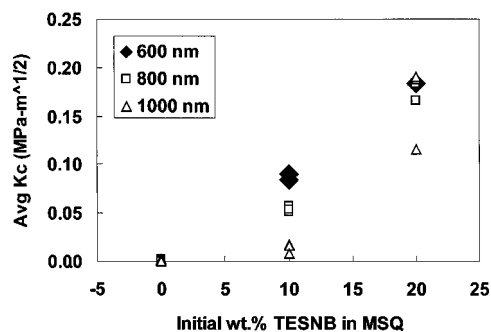


Figure 4. Plot of the average fracture toughness as a function of the initial weight percent of TESNB in the film and the average thickness.

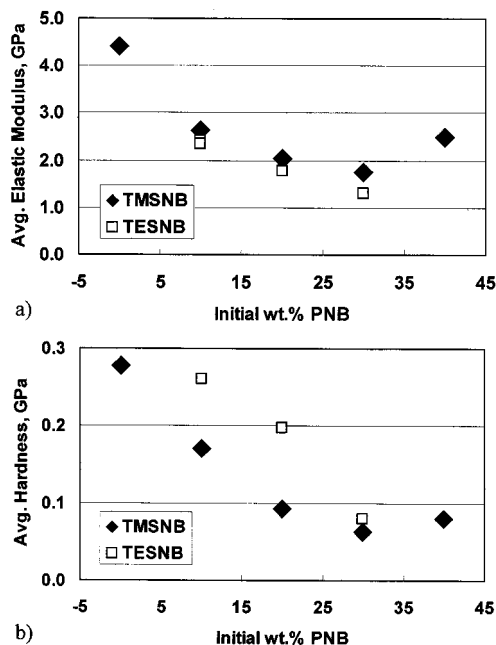


Figure 5. Plot of (a) average elastic modulus, and (b) average hardness as a function of the initial weight percent of TMSNB or TESNB in the films.

cracks.^{13,14} Mechanical properties (*i.e.*, E and H for fracture toughness) were measured with a Berkovich indenter as described below. Equation 1 relates the fracture toughness (K_c) measured in $\text{MPa}\cdot\text{m}^{1/2}$, to the length of the radial cracks (c) propagating from the corners of the impressions.

The results show a 10-fold increase in the fracture toughness with a 10 wt % increase in the concentration of sacrificial polymer in the film. Crack propagation is terminated at the boundary of a defect, or in the case of porous MSQ, at the boundary of a pore. With higher porosity, the films are more relaxed and there are more boundaries for crack termination. Also, the elastic modulus of the porous films is lower, thus reducing the driving force for crack initiation.

Figure 5 shows the average elastic modulus (Fig. 5a) and the average hardness (Fig. 5b) plotted against the initial sacrificial content in the MSQ films. Each data point was an average over 10 indents. Figure 5 presents data comparing the effect of TMSNB and TESNB sacrificial systems. Because the porogen was removed, little difference was observed.

The elastic modulus for the material, E , was calculated from⁷

$$\frac{1}{E_r} = \frac{(1 - \nu^2)}{E} + \frac{(1 - \nu_i^2)}{E_i} \quad [2]$$

where ν is the Poisson's ratio for the material, E_i and ν_i are the elastic modulus and Poisson's ratio for the indenter, respectively, and E_r is the reduced modulus obtained from Eq. 3, the Sneddon stiffness equation⁷

$$E_r = \frac{S\sqrt{\pi}}{2\beta\sqrt{A}} \quad [3]$$

In Eq. 3, S is the elastic stiffness or the slope of the unload curve at the beginning of the unloading segment when only elastic recov-

ery is involved, β is a geometric tip factor, and A is the area of contact. For these experiments, a Berkovich tip was used with a β factor of 1.034, and the area of contact is an experimentally determined function of the plastic or the contact depth and the geometry of the indenter. This type of analysis is necessary to isolate the elastic part from the plastic deformation produced in the indentation process. The hardness for these films was calculated by dividing the peak indentation load by the area of contact ($H = P/A$).⁷

The results show that the elastic modulus and hardness decrease with increasing concentration of sacrificial material in the film or porosity. Also, the samples prepared from the two different sacrificial systems (TMSNB and TESNB) show similar mechanical properties. The average elastic modulus was reduced from 4.41 GPa for a nonporous MSQ film to 1.76 GPa for a film with 30:70 wt % TMSNB:MSQ, and 1.30 GPa for a TESNB:MSQ film. A similar behavior is observed for the hardness, where the values were reduced from 0.28 GPa for an MSQ film, to 0.06 and 0.08 GPa for a 30:70 wt % TMSNB:MSQ, and 30:70 wt % TESNB:MSQ films, respectively. The differences between the 10 and 20 wt % TMSNB and TESNB samples could be indications of the differences in the microstructure of the pores, and further investigation is required.

Conclusions

A high degree of porosity can be achieved by bonding the sacrificial material to the spin-on glass matrix. Films with porogen loadings of up to 40 wt % have been fabricated without agglomeration or phase separation of the sacrificial polymer. Significant improvement in the fracture toughness of the films, and a slight decrease in the elastic modulus and the hardness were observed with increasing porosity. The index of refraction and the dielectric constant also decrease with porosity.

Acknowledgment

The experimental contributions of Prasad Shetty are greatly appreciated. L.R. acknowledges the sponsorship of the Assistant Secretary for Energy Efficiency and Renewable Energy, Office of Transportation Technologies, as part of the High Temperature Materials Laboratory User Program, Oak Ridge National Laboratory, managed by UT-Battelle, LLC, for the U.S. Department of Energy under contract No. DE-AC05-00OR22725.

The Georgia Institute of Technology assisted in meeting the publication costs of this article.

References

1. *International Technology Roadmap for Semiconductors*, Semiconductor Industry Association, San Jose, CA (2000).
2. L. Peters, *Semicond. Int.*, **23**, 108 (2000).
3. J. L. Hedrick, R. D. Miller, C. J. Hawker, K. R. Carter, W. Volksen, D. Y. Yoon, and M. Trollsas, *Adv. Mater.*, **10**, 1049 (1998).
4. D. Bhusari, H. Reed, M. Wedlake, A. Padovani, S. A. Bidstrup, and P. Kohl, *J. Microelectromech. Syst.*, In press.
5. A. T. Kohl, R. Mimna, R. Shick, L. Rhodes, Z. L. Wang, and P. A. Kohl, *Electrochem. Solid-State Lett.*, **2**, 77 (1999).
6. Allied Signal Advanced Microelectronic Materials, *Accuspin T-18 Flowable Spin-On Polymer (SOP)*, Product bulletin (1997).
7. W. C. Oliver and G. M. Pharr, *J. Mater. Res.*, **7**, 1564 (1992).
8. D. W. Gidley, W. E. Frieze, T. L. Dull, J. Sun, A. F. Yee, C. V. Nguyen, and D. Y. Yoon, *Appl. Phys. Lett.*, **76**, 1282 (2000).
9. M. P. Petkov, M. H. Weber, K. G. Lynn, K. P. Rodbell, and S. A. Cohen, *J. Appl. Phys.*, **86**, 3104 (1999).
10. N. Jayasundere and B. V. Smith, *J. Appl. Phys.*, **73**, 2462 (1993).
11. Y. Xu, Y. Tsai, K. N. Tu, B. Zhao, Q. Z. Liu, M. Brongo, G. T. T. Sheng, and C. H. Tung, *Appl. Phys. Lett.*, **75**, 853 (1999).
12. C. Nguyen, C. J. Hawker, R. D. Miller, E. Huang, J. L. Hedrick, R. Gauderon, and J. G. Hilborn, *Macromolecules*, **33**, 4281 (2000).
13. B. R. Lawn, A. G. Evans, and D. B. Marshall, *J. Am. Ceram. Soc.*, **63**, 574 (1980).
14. D. S. Harding, W. C. Oliver, and G. M. Pharr, *Mater. Res. Soc. Symp. Proc.* **356**, 663 (1995).